Fast Acquisition Techniques for Very Long PN Codes for On-Board Secure TTC Transponders

L.Simone, G.Fittipaldi
Radio Communication equipment Department
Thales Alenia Space Italy (TAS-I)
Rome, Italy
lorenzo.simone@thalesaleniaspace.com
giuseppe.fittipadi@thalesaleniaspace.com

I. Aguilar Sanchez
Electrical Systems Department
European Space Agency (ESA)
Noordwijk, The Netherlands
ignacio.aguilar.sanchez@esa.int

***Abstract*— Next generation of On-Board Telemetry, Tracking and Command (TTC) equipment for Secure Communications, based on Spread Spectrum Systems, shall adopt very long Pseudo Noise (PN) Cryptographic Codes in order to increase the Secure Satellite link Confidentiality and Anti-Jamming performances. This paper presents a new On Board PN Codes Synchronizer Architecture based on the Generalized Zero Padding Algorithm (GZP) and frequency domain Doppler compensation scheme in order to acquire very long PN codes at low Signal to Noise Ratio, large Doppler and large Jammer over Signal Power Ratio (J/S). It is shown that by adjusting the zeros padded to the received signal, the non coherent integrations and the Doppler compensation strategy, the On-Board Code Synchronizer satisfies all different satellite mission scenarios (Geo Stationary Orbit, Low Earth Orbit, Medium Earth Orbit and Launch and Early Orbit phases) requirements for very long PN code synchronization, ensuring very low code acquisition time due to the high parallel searching capability.**

Keywords-component*— *Detection Perfornace ,Acquisition time, Long PN Codes, Generalized Zero Padding scheme,Geo Stationary Orbit, Medium Earth Orbit, Low Earth Orbit, Anti Jamming.

I. INTRODUCTION

Secure Telemetry, Tracking and Command (TTC) link for satellite application may be threatened by intentional strong interferences or Cryptographic attack. In order to improve, the anti jamming and Transmission Security (TRANSEC) performances, very long Cryptographic Pseudo Noise (PN) codes can be exploited.

Time-domain Code Acquisition Techniques are often unsuitable to acquire a long PN Code in a short time. Generally, fully parallel acquisition algorithms show a huge hardware complexity, becoming not viable for Spaceborne Transponder design. Frequency-domain Code Acquisition algorithms show, instead, inherent parallel searching capability jointly with high detection performance also in a very hostile environment, characterized by large Doppler and Doppler rate and large Jammer-over-Signal Power ratio (J/S), up to 30dB. In [1], the Generalized Zero Padding Algorithm (GZP) is detailed and analyzed in presence of very low frequency Doppler and without interfering signals. In [2], an efficient carrier frequency Doppler-compensation technique in frequency domain is presented for low Doppler effect.

In the following sections, a new on board Code Synchronizer Architecture, based on the GZP algorithm and frequency domain Doppler-compensation technique, is described.

Our approach holds the main advantages of [1] and [2], but code synchronization performances are further enhanced exploiting a serial-over-time Doppler compensation scheme and an efficient jammer mitigation algorithm in order to cope a very large J/S (up to 30dB). Moreover, unlike [1] and [2], the Code Synchronizer Architecture is fully optimized, minimizing the hardware complexity, for different satellite mission scenarios: Geo Stationary Orbit (GSO), Medium Earth Orbit (MEO) and Low Earth Orbit (LEO).

The proposed on-board Code Synchronizer Architecture allows exploiting a Direct Sequence-Secure Spread Spectrum TTC link [3]-[5], characterized by very long PN codes, not only for the GSO mission but also for MEO, HEO and LEO missions, affected by large up link carrier frequency Doppler, ensuring high anti jamming performances and very low code acquisition time.

Section II briefly introduces the reference existing code acquisition techniques [2], section III details our proposed Code Synchronizer Architecture, section IV, dealing with the suitable algorithm optimization based on different satellite mission scenarios, provides numerical results, showing the performances of the proposed on board synchronizer architecture. Finally, section V concludes the paper.

II. FAST CODE ACQUISITION TECHNIQUES

A. *Generalized Zero Padding Code Acquisition Scheme*

In [1], the Zero Padding code acquisition algorithm [6]-[7] is improved optimizing the "zero padding" length based on the input Signal-to-Noise ratio (SNR). The core of the GZP algorithm is the Generalized Zero Padding Scheme (GZPS) that accomplishes to the following tasks: (a) group N-L incoming samples, (b) pad L samples to the (N-L) received samples to generate a block samples of length N, (c) perform

978-1-4673-0081-0/11/$26.00 ©2011 IEEE

the Fast Fourier Transform (FFT) and complex conjugation, (d) multiply the FFT results of (c) with the FFT results of N local code samples, (e) perform the Inverse Fast Fourier Transform (IFFT) of the above multiplication results (d), the first L+1 samples of the IFFT results represent the correlation of the N-L received samples and the N local code samples. After performing the IFFT output non coherent integrations, the result is compared with a pre defined code acquisition threshold, if the highest correlation peak is larger than the threshold, the code acquisition is declared, otherwise, a shift of L+1 samples is performed on the local PN code generator and the processing starts again from (a). Fig.1 shows the signal processing outlined above:

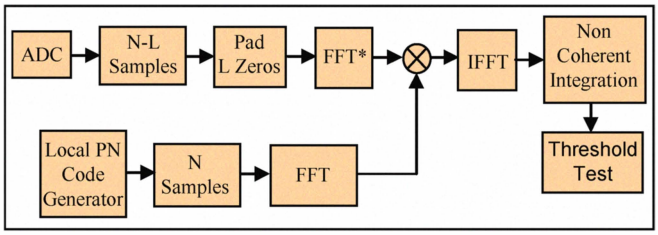

Figure 1. Generalized Zero Padding Scheme

The algorithm is able to check L+1 different code phases in parallel with low hardware complexity. The algorithm key parameters are: N, L and the non-coherent integration length. N fixes the FFT and IFFT size, the larger is N the larger is the hardware complexity. The zero padding length L is related to different opposed main aspects: increasing L the parallel searching capability increases, increasing L the detection performance [1] decreases, increasing L the detection performance degradation due to frequency Doppler effect decreases, that is, the coherent integration time decreases.

B. *Doppler Compensation in Frequency Domain*

Carrier frequency Doppler can be easily compensated in frequency domain [8] exploiting the Fourier Transform property:

$$x(t)\times e^{-j2\cdot\pi i\cdot f_d\cdot t} \Leftrightarrow X(f+f_d) \tag{1}$$

where x(t) is the original received signal, f_d is the frequency Doppler offset and X(f) is the Fourier Transform of x(t).

In discrete time domain, the carrier frequency Doppler offset can be compensated by a Discrete Time Fourier Transform (DTFT) circular rotation:

$$x(i)\times e^{-j\frac{2\pi}{N}id} \Leftrightarrow X\langle(k+d)\rangle_N \tag{2}$$

where N is the FFT length, d is the Doppler amount and $\langle\ \rangle_N$ indicates the modulus N circular rotation. Eq. (2) implies that, in frequency domain, x(i) multiplied by the local oscillator is equivalent to a circular rotation (modulus N) of X(f). Based on

(2), the FFT circular rotation can be exploited to compensate the carrier frequency Doppler offset, the resulting compensation resolution is given by:

$$\Delta_f = \frac{1}{NT_S} \tag{3}$$

where Ts stands for the sampling period. The correlation loss (L_{dop}) due to the uncompensated carrier frequency Doppler is determined by[9]:

$$L_{dop} = \mathrm{sinc}^2\left(\pi f_{dop} T_{CI}\right) \tag{4}$$

where sinc(x) represents sin(x)/x and T_{CI} is the pre detection coherent integration time.

III. ON BOARD CODE SYNCHRONIZER ARCHITECUTRE

A. *On Board Code Acquisition Signal Processing*

The new proposed Code Synchronizer Architecture is a fully reconfigurable platform which can be adopted for different satellite mission scenarios plainly adapting its key parameters.

Fig.2 shows the top level Synchronizer Architecture block diagram. The on-board synchronizer signal processing is based on a Sub-Sampling Receiver scheme which allows adopting low sampling frequency (F_S). The Synchronizer Architecture exploits only two samples per chip on the In-phase (I) and Quadrature (Q) channels; the intermediate frequency (F_{IF}), the sampling frequency and the code rate R_C are characterized by the following relationship:

$$F_{IF} = F_{OUT} + nF_s \tag{5}$$

where F_{OUT} is the lowest frequency digital signal spectrum replica due to the adopted sub-sampling scheme, n is an integer larger than 1, F_S is the sampling frequency and:

$$F_{OUT} = \frac{F_S}{4} = R_C \tag{6}$$

Being *Fs* four times F_{OUT}, the Quarter Rate Translation[10] is pursued to down-convert the digital signal centered at F_{OUT} (ADC output) to the base band fully in digital domain without any additive mixer (the quarter rate translation jointly with the I and Q components extraction are performed by the Digital Front-End). Based on (5) and (6), the band pass spread spectrum signal from F_{IF} is down-converted first to F_{OUT} and than to base band, fully in digital domain without any additional mixer. On the I and Q channels, N-L received samples are grouped and padded by L zeros in order to generate a single Up-Link signal block of length N. The In-phase and Quadrature up link signal block are summed term by term in order to generate the "Up Link Complex Signal. The complex conjugate N-point FFT is performed on the up-link complex signal, followed by the Doppler compensation processing (if needed). The local PN code generator output samples are grouped in a single block of length N followed by the FFT processing. The multiplication between the Doppler compensation output and the local N-point FFT output are performed and followed by the complex IFFT.

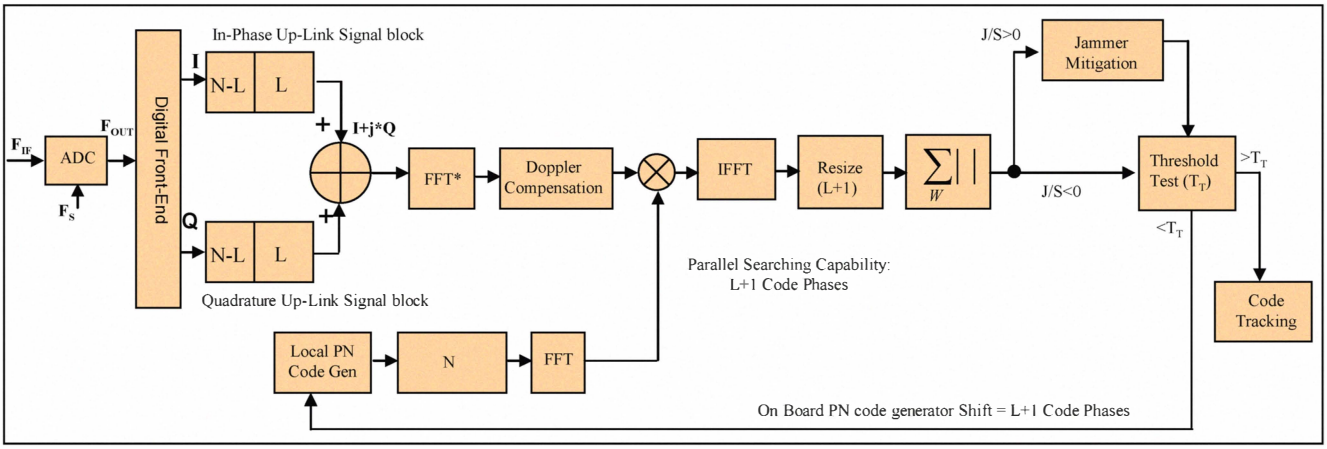

Figure 2. On Board Code Synchronizer Architecture – top level block diagram

The IFFT output vector of length N is resized to L+1; only the first L+1 samples are preserved discarding the others; the first L+1 samples represents a single observation window, that is, the parallel searching capability. Following, non coherent integration process is performed, the absolute value of W (non coherent integration length) vectors of length N are added term-by-term. The Non Coherent Integrator (NCI) output feeds the Jammer Mitigation (JM) Algorithm before threshold comparison if the jammer is detected (exploiting dedicated algorithms) or directly the threshold comparison block if only the useful signal is present. Before comparing the NCI output or the JM algorithm output with the pre-defined acquisition threshold, the mean value of the NCI output block is subtracted from itself, this operation makes the detection algorithm more robust against large J/S value. If the correlation peak is larger than the pre-defined Threshold (T_T), the code alignment is declared and the code tracking loop is activated, otherwise, if the correlation peak is lower than T_T, the local PN code generator is shifted by L+1 samples and the same process is performed again until the code acquisition is declared.

The above architecture tests L+1 code phases in parallel. The exact incoming code phase with respect to the on board one is detected according to the index position of the correlation peak on the NCI output vector of length L+1.

For the GSO, MEO and LEO mission scenarios, L lives in the range 6000÷7500 samples while N=8192 samples, this means that the above Synchronizer Architecture tests up to 7500 different code phases in parallel which leads to a very impressive code acquisition time, allowing the acquisition of a very long PN code in a short time.

B. *Enhanced Carrier Frequency Doppler Compensation Scheme*

Some satellite mission scenario like MEO and LEO are characterized by a very large up link carrier frequency Doppler offset up to ± 57kHz (LEO). In order to acquire a long PN code also in this hostile scenario, a Doppler compensation processing is required. In order to keep down the hardware complexity, the up link carrier frequency Doppler is compensated serially over time. In different time intervals, a different code frequency Doppler is compensated by a suitable rotation of the FFT* output. The whole carrier frequency Doppler offset is partitioned into m different "Doppler Sub Ranges" based on the maximum uncompensated Doppler offset which leads to a negligible detection probability degradation due to the correlation loss (4). Before discarding the nth observation window shifting the on board PN code generator by L+1 code phases, each Doppler sub range must be explored rotating the FFT* output by a suitable amount of samples based on the central frequency of the current Doppler sub range.

Exploiting the above Doppler compensation scheme, only the Doppler effect on the up link carrier frequency is compensated leaving unchanged the code Doppler effect. In order to avoid the code correlation loss due to the real time codes sliding caused by the code Doppler effect, it's necessary to keep down to ¼ chip time (T_C) the code sliding amount, keeping down to a specific value the maximum non coherent integration length W^*:

$$W^* = \left\lfloor \frac{F_S \cdot F_C}{2 \cdot (N - L) \cdot \Delta f \cdot 4 \cdot R_C} \right\rfloor \qquad (7)$$

where F_C is the up link carrier frequency, and Δf is the overall up link carrier frequency Doppler offset. Keeping down to W^* the non coherent integration length, the code rate Doppler effect can be neglected.

C. *Jammer Mitigation Processing*

If an intentional CW interference characterized by large J/S affects the spread spectrum signal bandwidth, taking into account that the worst case condition happens when the jammer frequency is the same of the useful signal one, the NCI output, that is, the codes correlation results, can be completely destroyed disabling the peak detection capability.

The aim of the jammer mitigation algorithm is to decorrelate the jammer power leaving unchanged the signal correlation properties. If the jammer is detected, what is compared with the pre defined threshold is the first derivative of the NCI output instead of the NCI output. When the codes are aligned, the correlation peak is well detectable, while the jammer waveform is decorrelated by the first derivate processing.

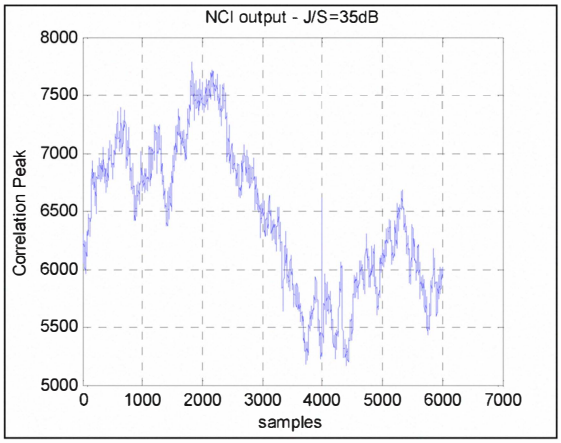

Figure 3. Correlation Output before Jammer Mitigation processing

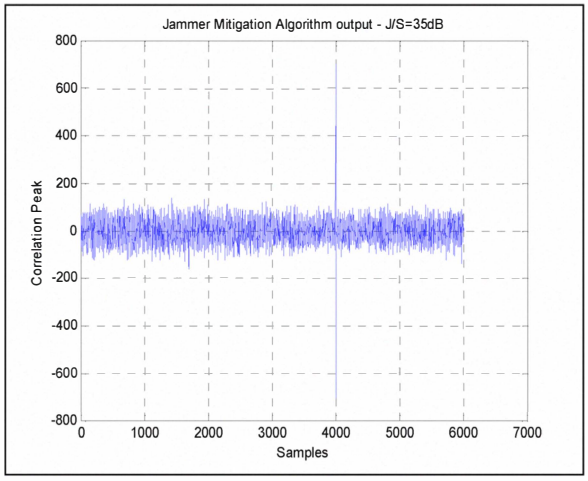

Figure 4. Jammer Mitigation processing outoput

Fig. 3 and Fig. 4 show respectively the correlation results before and after the jammer mitigation processing when the simulated phase misalignment between the up link code and the on board one is 4000 samples, that is, 2000 chips and J/S=35dB. In Fig. 3 the correlation peak is completely drowned by the corrupted correlation samples due to the jammer effect; the correlation peak is undetectable. In Fig. 4 instead, the correlation peak is well detectable while the jammer waveform is completely decorrelated.

IV. CODE SYNCHRONIZER OPTIMIZATION FOR DIFFFERENT SATELLITE MISSION SCENARIOS AND NUMERICAL RESULTS

The proposed On-Board Code Synchronizer Architecture depicted in Fig. 2 can be used for acquiring a long PN code, (code length up to 2^{26} chips) for different satellite mission scenarios, by way of example: GSO, MEO and LEO. Tab. I highlights the main satellite "Secure TTC Link" radio frequency (RF) requirements, based on specific link analysis for each different mission scenarios:

TABLE I. SECURE TTC LINK - KEY RADIO FREQUENCY REQUIREMENTS

Mission Scenario	Up Link Carrier Frequency [MHz]	Code Rate [MCps]	SNR [dB]	J/S [dB]	Carrier Doppler Range [±Hz]	Carrier Doppler Rate [±Hz/s]	Data Rate [bps]
GSO	40	10	-27	30	1800	5	10000
MEO	2034,747	3	-9,78	27	8000	10	2000
LEO	2254,1	3	11,22	27	57000	700	2000

The overall up-link carrier frequency Doppler and Doppler rate are characterized by huge margins, taking into account the on-board local oscillator (LO) frequency instability and no Doppler pre-compensation by the Ground Station.

Tab. II highlights the code acquisition architecture key parameters optimization for GSO, MEO and LEO scenarios in order to meet the Secure TTC Link requirements detailed in Tab. I.

To enhance the code detection performance, the code synchronizer architecture, fully reconfigurable, has been optimized differently for "Nominal Mode" (only the useful up-link signal is present) and for "Stress Mode" (a jammer signal affects the useful TTC signal). The On Board Spread Spectrum Transponder exploits specific jammer detection algorithms to set the Nominal Mode configuration or the Stress mode one.

Fig. 5-Fig.13 show respectively, for GSO, MEO and LEO mission scenarios: the Code acquisition probability (Pd) versus input Signal over Thermal Noise Power Spectral Density Ratio (S/No); the Average Code Acquisition Time versus input S/No for different PN code lengths and the Code Acquisition Probability (Pd) versus input Jammer over Signal power Ratio (J/S).

Tab. III summarizes the Code Acquisition Time performances for different code lengths, based on the RF environment requirements detailed in Tab. I.

TABLE II. ON BOARD CODE SYNCHRONIZER ARCHITECTURE OPTIMIZATION FOR DIFFERENT SATELLITE MISSION SHENARIOS

Mission Scenario	Intermediate Freqeuncy F_{IF} [MHz]	Sampling Freqeuncy F_S [MHz]	Code Rate R_c [MCps]	N [samples]	L [samples]	W (Nominal Mode)	W (Stress Mode)	Doppler sub ranges (Nominal Mode)	Doppler sub-ranges (Stress Mode)
GSO	130	40	10	8192	6000	25	30	1	1
MEO	135	12	3	8192	6200	4	20	5	5
LEO	135	12	3	8192	7300	5	5	7	25

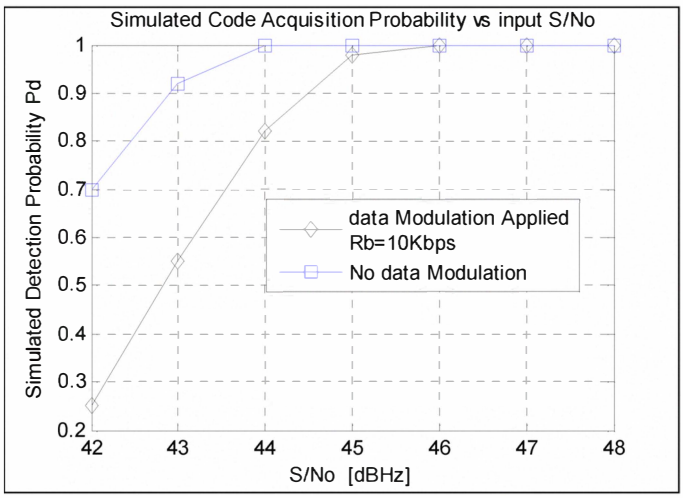

Figure 5. GSO Mission – Detection Probability vs input S/No, Up Link Carrier Frequency doppler f_d=1.8KHz.

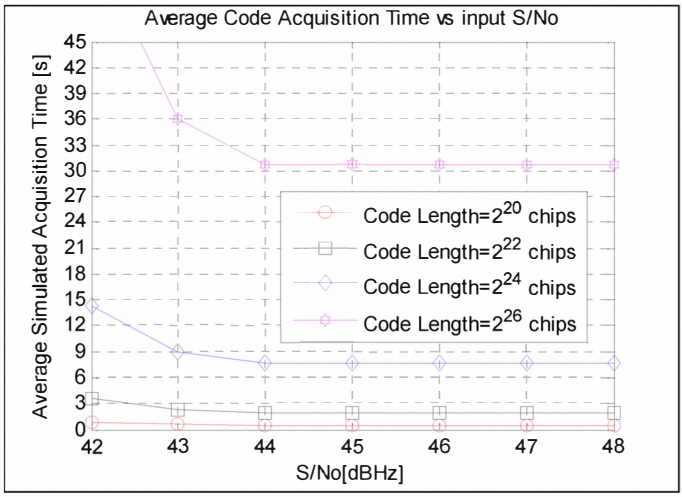

Figure 6. GSO Mission – Code Acquisition Time vs input S/No, Up Link Carrier Frequency doppler f_d=1.8KHz.

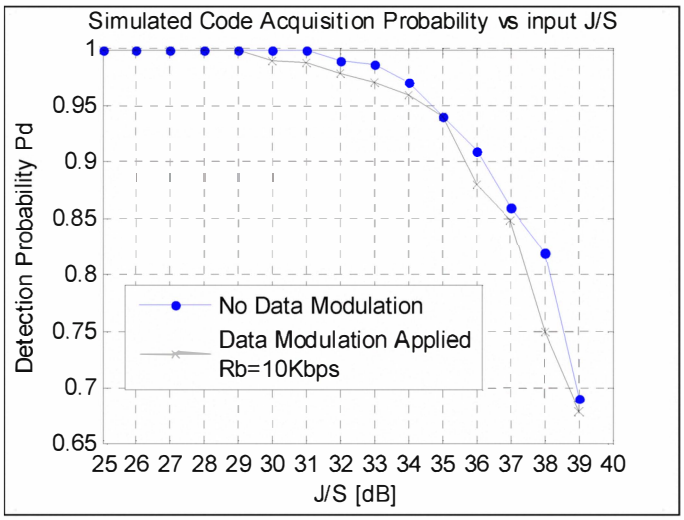

Figure 7. GSO Mission –Detection Probability vs input J/S, Up Link Carrier Frequency doppler f_d=1.8KHz, Jammer frequency equal to the useful signal frequency, S/N_0=60dBHz.

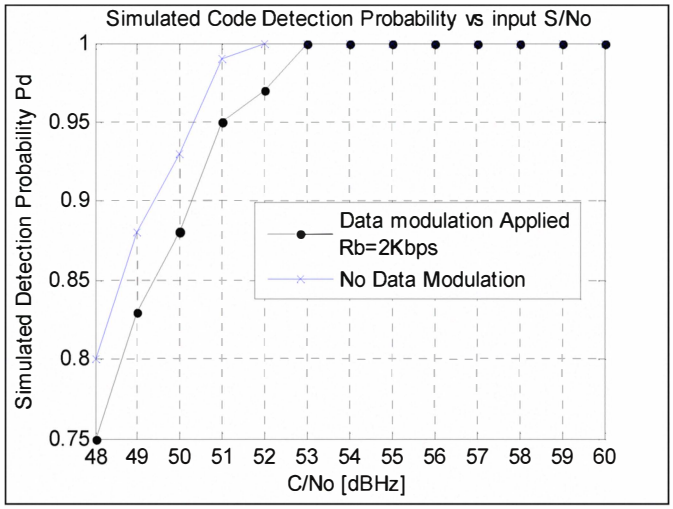

Figure 8. MEO Mission – Detection Probability vs input S/No, Up Link Carrier Frequency doppler f_d=8KHz.

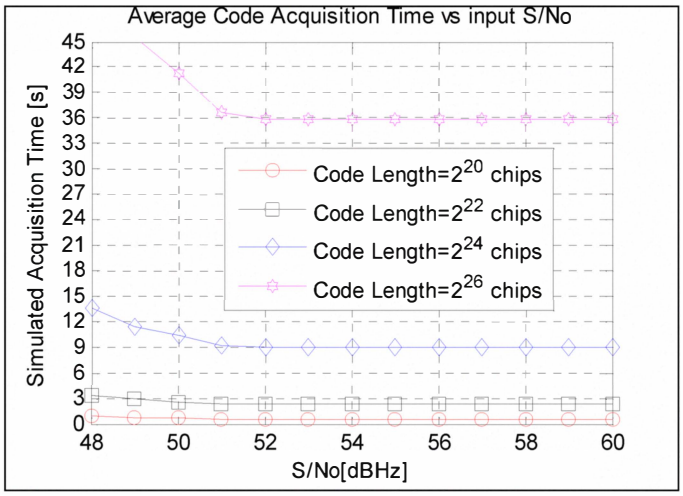

Figure 9. MEO Mission – Code Acquisition Time vs input S/No, Up Link Carrier Frequency doppler f_d=8KHz.

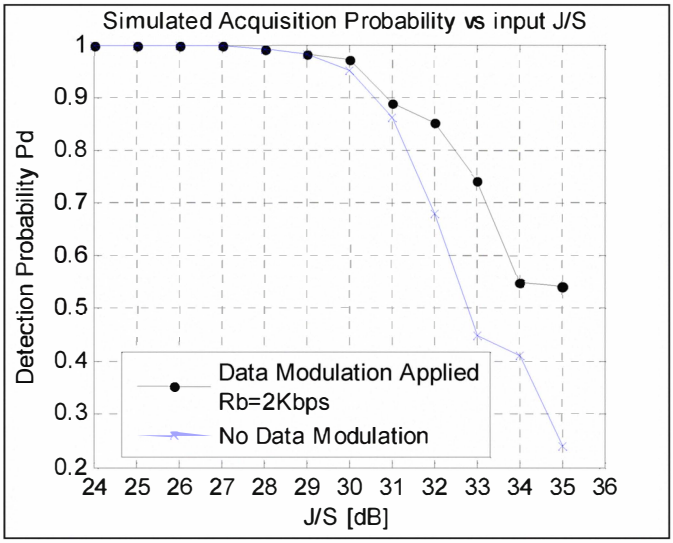

Figure 10. MEO Mission –Detection Probability vs input J/S, Up Link Carrier Frequency doppler f_d=8KHz, Jammer frequency equal to the useful signal frequency, S/N_0=60dBHz.

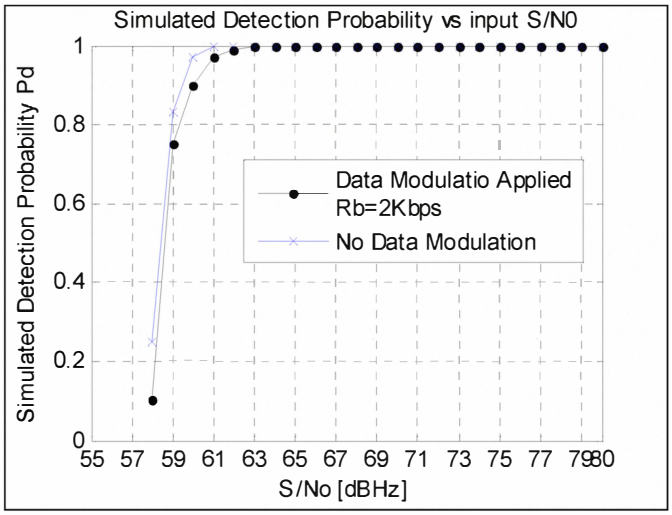

Figure 11. LEO Mission – Detection Probability vs input S/No, Up Link Carrier Frequency doppler f_d=57KHz.

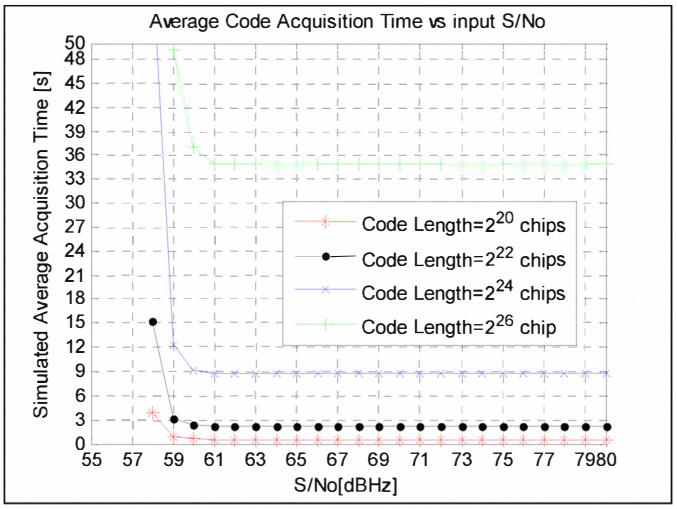

Figure 12. LEO Mission – Code Acquisition Time vs input S/No, Up Link Carrier Frequency doppler f_d=57KHz.

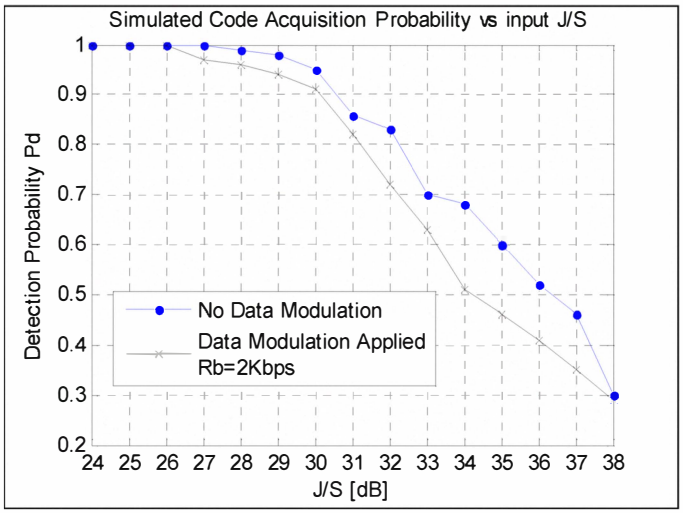

Figure 13. LEO Mission –Detection Probability vs input J/S, Up Link Carrier Frequency doppler f_d=57KHz, Jammer frequency equal to the useful signal frequency,S/N_0=60dBHz

TABLE III. SYNCHRONIZER ARCHITECTURE CODE ACQUISITION TIME SUMMARY VS CODE LENGTH

Synchronizer Architecture - Code Acquisition Time (P_d>99,9%,P_{fa}<10^{-5})								
Mission Scenario	$L_{Code}=2^{20}$		$L_{Code}=2^{22}$		$L_{Code}=2^{24}$		$L_{Code}=2^{26}$	
	Max [s]	Average [s]	Max [s]	Average [s]	Max [s]	Average [s]	Max [s]	Average [s]
GSO	0,94	0,47	3,82	1,91	15,32	7,66	61,14	30,57
MEO	2,24	1,12	8,98	4,49	35,9	17,95	143,7	71,85
LEO	5,35	2,67	2135	10,67	85,5	42,75	341,6	170,81

L_{code}=Code Length [chips]

V. CONCLUSIONS

In this paper, a novel On-Board PN Code Synchronizer Architecture for GSO, MEO and LEO satellite mission scenarios-Spread Spectrum Secure TTC link has been presented. The proposed approach allows detecting the incoming PN code in a very hostile environment characterized by large Doppler up to 57kHz (LEO) and large jammer-over-signal power ratio up to 32dB (GSO) and it allows using very long up link PN code (up to $2^{24}\div2^{26}$ chips) while ensuring quite short acquisition time. Finally, the selected Code Synchronizer allows increasing the Anti-Jamming and Confidentiality performances of the Secure TTC link, not only for standard GSO mission but also for more challenging MEO and LEO scenarios.

ACKNOWLEDGMENT

This work has been supported by ESA Project AO/1-5940/08/NL/JK "Cryptographic Pseudo-noise codes and related acquisition techniques for direct-sequence spread-spectrum transponders".

REFERENCES

[1] H. Li, X. Cui, M. Lu, and Z. Feng, *"Generalized Zero-Padding Scheme for Direct GPS P-Code Acquisition", IEEE Transactions on Wireless Communications*, vol. 8, no. 6 June 2009.

[2] J. L. Hong, L. Mingquan, F.Zhenming, "Direct GPS P-Code Acquisition Method Based on FFT", *Tsinghua Science and Technology,* issn 1007-0214 02/19 pp9-16, volume 13, Number 1, February 2008.

[3] I. S. J.K. Holmes, "Coherent Spread-Spectrum Systems", J. Wiley, 1982..

[4] D.J.Torrieri, "Performance of Direct-Sequence Systems with Long Pseudonoise Sequences,"IEEE Journal on Selected Areas in Communications. VOL.10, NO.4, May 1992.

[5] M. K. Simon, J. K. Omura, R.A. Scholtz, B.K. Levitt, *Spread Spectrum Communications Handbook*, McGraw-Hill.

[6] D. M. Lin and J. B. Y. Tsui, "Acquisition through circular correlation by partition for GPS C/A code and P(Y) code," US patent No 6567042, May, 2003.

[7] A. Jovancevic, S. Ganguly, and S. Zigic, "Direct P(Y)/M-code acquisition" in Proc. ION GNSS, Long Beach, CA, 2004, pp. 561–572.

[8] Yang C, Vasquez M J, Chaffee J. Frequency-domain Doppler search and jamming suppression for fast direct P(Y)- code acquisition. In: Proceedings of ION GPS. Nashville, USA, 1999: 1157-1167.

[9] Wolfert R, Chen S , Kohli S, Leimer D, Lascody J. Direct P(Y)-code acquisition under a jamming environment. In: Position Location and Navigation Symposium. Palm Springs, USA, 1998:228-235

[10] R.G. Lyion, *Understanding Digital Signal Processing*, McGraw-Hill.